ARTHRITIS & RHEUMATOLOGY
Vol. 66, No. 6, June 2014, pp 1648–1658
DOI 10.1002/art.38409

Epigenome-Wide Scan Identifies a Treatment-Responsive Pattern of Altered DNA Methylation Among Cytoskeletal Remodeling Genes in Monocytes and CD4+ T Cells From Patients With Behçet's Disease

Travis Hughes,[1] Filiz Ture-Ozdemir,[2] Fatma Alibaz-Oner,[2] Patrick Coit,[1] Haner Direskeneli,[2] and Amr H. Sawalha[1]

Objective. **The pathogenesis of Behçet's disease (BD), an inflammatory disease with multisystem involvement, remains poorly understood. This study was undertaken to investigate whether there are DNA methylation abnormalities in BD that might contribute to the pathogenesis of the disease.**

Methods. **We examined genome-wide DNA methylation patterns in monocytes and CD4+ T cells from 16 male patients with untreated BD and age, sex, and ethnicity–matched healthy controls. Additional samples were collected from 12 of the same BD patients after treatment and achievement of disease remission. Genome-wide DNA methylation patterns were assessed using the Infinium HumanMethylation450 BeadChip array, which includes >485,000 individual methylation sites across the genome.**

Results. **We identified 383 CpG sites in monocytes, and 125 in CD4+ T cells, that were differentially methylated between BD patients and controls. Bioinformatic analysis revealed a pattern of aberrant DNA methylation among genes that regulate cytoskeletal dynamics, suggesting that aberrant DNA methylation of multiple classes of structural and regulatory proteins of the cytoskeleton might contribute to the pathogenesis of BD. Further, treatment of BD modified the differences in DNA methylation observed in patients compared to controls; indeed, among CpG sites that were differentially methylated after disease remission versus before treatment, there was widespread reversal of the direction of aberrant DNA methylation observed between the patient and control groups.**

Conclusion. **The results of this epigenome-wide study—the first such study in BD—provide strong evidence that epigenetic modification of cytoskeletal dynamics underlies the pathogenesis of BD and its response to treatment.**

Behçet's disease (BD) is an inflammatory disease characterized by the presence of recurrent oral and genital ulcers, skin lesions, and uveitis. Mucocutaneous lesions in BD typically exhibit leukocyte infiltration, primarily by T cells and monocytes (1). Widespread enhancement of leukocyte motility and tissue infiltration occurs in BD. Monocytes from patients with BD display increased activity and promote increased neutrophil adhesion (2). Further, levels of macrophage inflammatory protein 1α, which promotes lymphocyte chemotaxis, are elevated in BD (3). Activated CD4+ T cells play a critical role in BD pathogenesis, and an expansion of Th17 cells via interleukin-21 signaling and increased levels of γ/δ T cells are observed (4–6).

Endothelial cell injury is common in BD. Levels of soluble E-selectin molecules have been reported to be increased in the serum of patients with active disease (7). Vascular endothelial cell function becomes impaired in response to oxidative damage (8). Disruption of tight junctions between endothelial cells is mediated by changes in class II myosin phosphorylation and remod-

Supported by the Rheumatology Research Foundation (Rheumatology Investigator award to Dr. Sawalha) and the NIH (grant P30-ES-017885 to Dr. Sawalha).

[1]Travis Hughes, MPH, Patrick Coit, BSc, Amr H. Sawalha, MD: University of Michigan, Ann Arbor; [2]Filiz Ture-Ozdemir, PhD, Fatma Alibaz-Oner, MD, Haner Direskeneli, MD: Marmara University School of Medicine, Istanbul, Turkey.

Address correspondence to Amr H. Sawalha, MD, Division of Rheumatology, Department of Internal Medicine, University of Michigan, Room 5520 MSRB-1, SPC 5680, 1150 West Medical Center Drive, Ann Arbor, MI 48109. E-mail: asawalha@umich.edu.

Submitted for publication October 10, 2013; accepted in revised form February 11, 2014.

eling of the F-actin cytoskeleton (9). Cytoskeletal remodeling in endothelial and immune cells accompanies lymphocyte adhesion and tissue infiltration in the normal inflammatory response (10). Treatments that disrupt microtubule processing might be effective in limiting the frequency and severity of mucocutaneous symptoms in BD, but their exact mechanism of action remains uncertain.

BD has a strong genetic component, as evidenced by the geographic concentration of the disease along the Old Silk Road (11). The most robust genetic association observed in BD to date is within the HLA region. Recent evidence suggests that there are multiple independent genetic susceptibility loci for BD in the HLA class I region, with the strongest effect localized to the genetic region between *HLA-B* and *MICA* (12). Multiple associations outside of the HLA region have also been reported in BD, including associations with *IL10*, *IL23R*, *UBAC2*, *STAT4*, *CCR1*, *KLRC4*, *ERAP1*, and *GIMAP2*/*GIMAP4* (13). While there is a strong genetic component to BD, genetic variation alone is not sufficient to explain the heritability and pathogenesis of the disease.

To date there have been no reported studies of the involvement of DNA methylation (the addition of a methyl group to the fifth carbon in cytosine rings within CpG dinucleotides) in BD. However, there is a growing body of evidence that changes in DNA methylation have an important role in multiple immune-mediated diseases (14–17). DNA methylation ex utero is primarily mediated by DNA methyltransferase 1 and is generally a repressive epigenetic mark. Hypermethylation of DNA results in transcriptional gene repression, while hypomethylation is associated with a chromatin configuration that is transcriptionally permissive (18).

Herein we report the results of an epigenome-wide study of the methylation status of >485,000 individual methylation sites across the genome, among treatment-naive BD patients and healthy matched controls. We also evaluated epigenome-wide DNA methylation status in individual BD patients before and after treatment with achievement of disease remission. We obtained evidence of widespread DNA methylation changes in BD across the genome. Our data suggest that DNA methylation changes in genes involved in cytoskeletal dynamics contribute to the pathogenesis of BD and that restoration of DNA methylation of microtubule-processing genes occurs following achievement of disease remission.

PATIENTS AND METHODS

Patient selection and sample collection. Sixteen male BD patients and 16 healthy controls matched for age (±5 years), sex, and ethnicity were recruited to participate in this study. All patients were recruited from the rheumatology clinics at Marmara University School of Medicine. Disease manifestations of the patients are reported in Supplementary Table 1 (on the *Arthritis & Rheumatology* web site at http://onlinelibrary.wiley.com/doi/10.1002/art.38409/abstract). All patients studied had either not received treatment for BD or had not received treatment for at least 3 months prior to enrollment, and samples were collected at the initial study visit. Samples were further collected from 12 of the 16 BD patients following treatment and achievement of disease remission (defined as the absence of any disease-associated symptoms or organ involvement for at least 1 month). The study was approved by the ethics committees and institutional review boards at Marmara University School of Medicine and the University of Michigan. All study participants provided written informed consent prior to enrollment.

Isolation of monocytes and CD4+ T cells and DNA extraction. Peripheral blood mononuclear cells (PBMCs) were isolated, by density-gradient centrifugation (Amersham Biosciences), from fresh blood samples obtained from BD patients and healthy controls. Monocytes and CD4+ T cells were purified from PBMCs by magnetic bead separation (Miltenyi Biotec). The purity of isolated cell populations, confirmed by flow cytometry using fluorochrome-conjugated antibodies against CD14 (for monocytes) and CD4 (for T helper lymphocytes), was >90% for both monocytes and CD4+ T cells. Genomic DNA was obtained from isolated monocytes and CD4+ T cells using a DNeasy Blood and Tissue Kit (Qiagen).

Genome-wide DNA methylation profiling. Bisulfite conversion was performed using an EZ DNA Methylation Kit (Zymo Research). Whole-genome amplification of bisulfite-converted DNA was performed prior to array hybridization. An Infinium HumanMethylation450 BeadChip array kit was used to assess the methylation status of >485,000 individual methylation sites throughout the genome. This array covers 99% of RefSeq genes, with an average of 17 CpG sites per gene across the promoter region, 5′-untranslated region (5′-UTR), first exon, gene body, and 3′-UTR. It also covers 96% of CpG islands. Non-CpG methylated sites recently identified in human stem cells are also covered, as are microRNA promoter regions.

Quality control, identification of differentially methylated CpG sites, and bioinformatic analysis. Comparisons of DNA methylation levels between BD patients and healthy controls were performed separately for monocytes and CD4+ T cells. Differences in DNA methylation associated with treatment for BD were also assessed separately in monocytes and CD4+ T cells. Differential methylation analysis was performed using the Genome Studio methylation package. Beta values were used to represent the percent methylation at each CpG site, and were calculated using the ratio of intensities between methylated and unmethylated alleles, as follows: β = methylated/(unmethylated + methylated + 100).

Methylation data were normalized in Genome Studio. Prior to analysis a total of 50,446 probes were removed due to the presence of single-nucleotide polymorphisms within 10

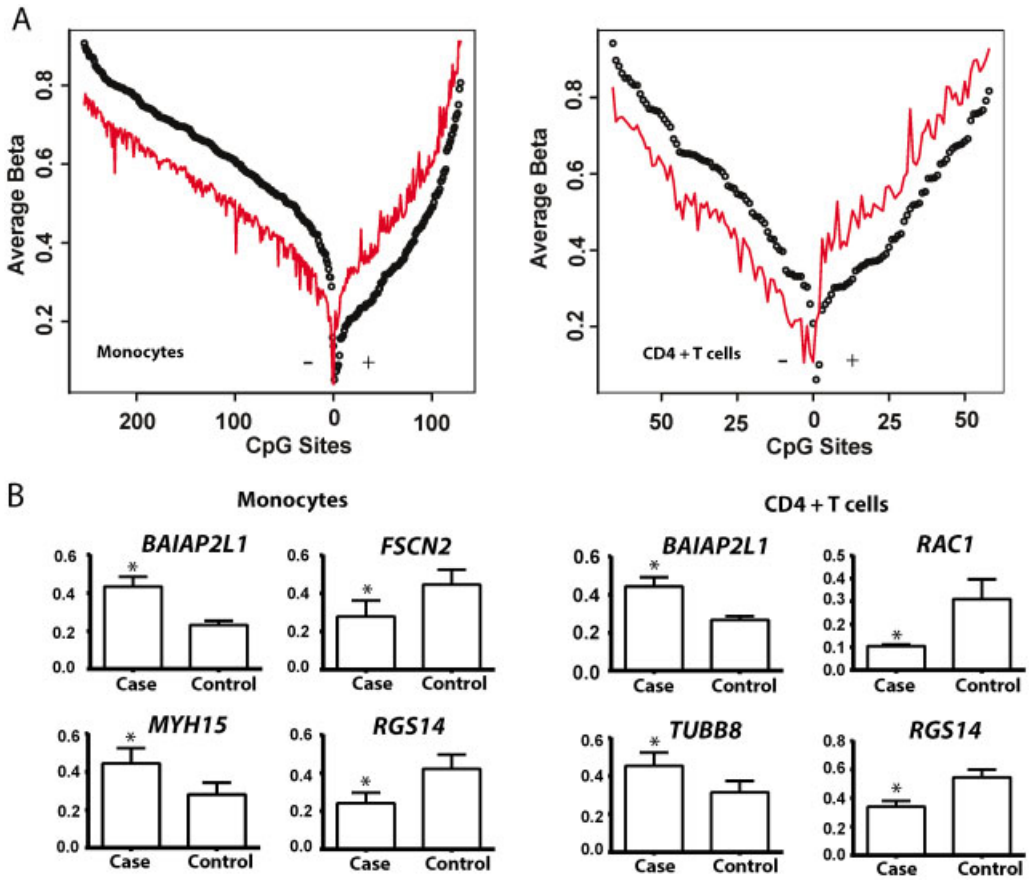

Figure 1. Differential methylation of CpG sites in monocytes and CD4+ T cells from patients with Behçet's disease (BD). **A,** Differential methylation in 16 male BD patients compared to 16 age, sex, and ethnicity–matched healthy controls. In monocytes, 383 CpG sites were differentially methylated, of which 254 were hypomethylated and 129 were hypermethylated. In CD4+ T cells, 125 CpG sites were differentially methylated, of which 67 were hypomethylated and 58 were hypermethylated. Within each panel, hypomethylated CpG sites are represented on the left and hypermethylated sites on the right. For each CpG site the average beta values, which represent the percent methylation, are shown (in red for BD patients; in black for controls). **B,** Differential methylation of a number of genes related to cytoskeletal dynamics in monocytes and CD4+ T cells from BD patients compared to controls. Values are the mean ± SEM fraction of methylation. $* = P < 0.01$ versus controls.

bases of the CpG target sequence. No probes were observed to have detection P values greater than 0.05. The P value for differential methylation between patients and controls was calculated using the following equation:

$$P = \mathrm{z}\left(\frac{|\beta_{\mathrm{patient}} - \beta_{\mathrm{control}}|}{\frac{s^2_{\mathrm{control}}}{N_{\mathrm{control}}} - \frac{s^2_{\mathrm{patient}}}{N_{\mathrm{patient}}}}\right)$$

where s is the standard deviation estimate and z is the 2-sided tail probability of the standard normal distribution. The standard deviation estimate s is a function of β and was calculated as $s = A\beta^2 + B\beta + C$, where $A = -0.1511$, $B = 0.1444$, and $C = 0.01646$. A, B, and C values were derived by Illumina by repeatedly measuring loci with known methylation fractions ranging from 0 to 1 and fitting a parabola to the standard deviation as a function of β. A differential methylation score (DiffScore) for each probe was calculated as follows:

$$\mathrm{DiffScore} = 10 \times \mathrm{sgn}(\beta_{\mathrm{patient}} - \beta_{\mathrm{control}}) \times -\log_{10}(P)$$

where $\mathrm{sgn}(i) = +1$ when $i > 0$, $\mathrm{sgn}(i) = 0$ when $i = 0$, and $\mathrm{sgn}(i) = -1$ when $i < 0$.

Probes with an average methylation difference ($\Delta\beta$) of at least 10% (BD patients versus controls) or 5% (patients before treatment versus patients after treatment) and differential methylation scores of at least 22 (equivalent to a differential methylation P value of ≤ 0.01), after adjustment for multiple testing using a Benjamini and Hochberg false discovery rate (FDR) of 5%, were considered differentially methylated. A linear regression model was fitted to estimate batch effect in differentially methylated loci using R, and no batch effect was detected in our study.

We performed bioinformatic analysis to identify canonical pathways and cellular processes that were enriched among differentially methylated CpG sites, through Gene Ontology (GO) analysis using DAVID software (19). We

Table 1. CpG sites that were differentially methylated in monocytes from Behçet's disease patients compared to monocytes from healthy controls*

Probe	Gene symbol	Gene name	Methylation (β), patients	Methylation (β), controls	$\Delta\beta$	P
Hypomethylated sites						
cg07211972	*CBS*	Cystathionine-β-synthase	0.374	0.604	−0.230	1.59×10^{-34}
cg15971518	*PRG2*	Proteoglycan 2, bone marrow	0.282	0.470	−0.187	6.85×10^{-25}
cg17509989	*RGS14*	Regulator of G protein signaling 14	0.242	0.421	−0.179	5.35×10^{-24}
cg16006841	*RGS14*	Regulator of G protein signaling 14	0.341	0.519	−0.178	4.67×10^{-21}
cg06060754	*RGS14*	Regulator of G protein signaling 14	0.315	0.488	−0.173	3.74×10^{-20}
cg05248234	*FSCN2*	Fascin homolog 2, actin-bundling protein, retinal	0.280	0.450	−0.170	2.97×10^{-20}
cg06559318	*HLA-DRB6*	Major histocompatibility complex, class II, DRβ6	0.282	0.444	−0.162	2.85×10^{-18}
cg05398700	*WDR20*	Tryptophan–aspartic acid repeat domain 20	0.644	0.805	−0.161	5.38×10^{-25}
cg23646109	*BCYRN1*; *GJB1*	Brain cytoplasmic RNA 1; gap junction protein, β1, 32 kd	0.751	0.907	−0.156	1.59×10^{-34}
cg17220055	*HIVEP3*	Human immunodeficiency virus type I enhancer binding protein 3	0.401	0.554	−0.153	7.7×10^{-15}
Hypermethylated sites						
cg08684580	*BAIAP2L1*	Brain-specific angiogenesis inhibitor 1–associated protein 2–like 1	0.434	0.234	0.200	8.89×10^{-35}
cg24634471	*JRK*	Jerky homolog (mouse)	0.630	0.434	0.195	8.89×10^{-35}
cg10596483	*JRK*	Jerky homolog (mouse)	0.522	0.349	0.172	8.89×10^{-35}
cg26053840	*GLO1*	Glyoxalase I	0.465	0.305	0.160	8.89×10^{-35}
cg17965159	*LRMP*	Lymphoid-restricted membrane protein	0.594	0.434	0.160	8.89×10^{-35}
cg03329597	*MYH15*	Myosin heavy chain 15	0.442	0.284	0.159	8.89×10^{-35}
cg07921503	*CHST12*	Carbohydrate (chondroitin 4) sulfotransferase 12	0.226	0.072	0.155	8.89×10^{-35}
cg10105218	*CD53*	CD53 molecule	0.397	0.249	0.149	8.89×10^{-35}
cg06915202	*BAIAP2L1*	Brain-specific angiogenesis inhibitor 1–associated protein 2–like 1	0.469	0.321	0.148	8.89×10^{-35}
cg14040931	*GNE*	Glucosamine (UDP-*N*-acetyl)-2-epimerase/*N*-acetylmannosamine kinase	0.488	0.342	0.146	8.89×10^{-35}

* The sites listed are those that were the most highly hypo- or hypermethylated in patients compared to controls.

examined enrichment among OMIM diseases, Kyoto Encyclopedia of Genes and Genomes pathways, PANTHER pathways, molecular function (MF), cellular component (CC), and biologic process (BP) gene ontology terms among differentially methylated gene sets. A background of all RefSeq genes was selected for GO analysis in DAVID. Network interaction analysis was performed using GeneMania (20).

RESULTS

Behçet's disease–associated differences in DNA methylation. We observed significant differences between BD patients and healthy controls in DNA methylation across the genome (Figure 1A). In monocytes, 383 CpG sites in 228 genes were differentially methylated between patients and controls, with 129 hypermethylated CpG sites and 254 hypomethylated sites (Table 1 and Supplementary Table 2 [on the *Arthritis & Rheumatology* web site at http://onlinelibrary.wiley.com/doi/10.1002/art.38409/abstract]). In CD4+ T cells, there were 125 differentially methylated CpG sites (67 hypomethylated and 58 hypermethylated) in 62 genes (Table 2 and Supplementary Table 3). While hypomethylation was more prevalent in monocytes, we observed a high degree of concordance between CD4+ T cells and monocytes in terms of differential methylation; indeed, 59 of the 125 CpG sites that were differentially methylated in CD4+ T cells from BD patients compared to controls were also differentially methylated in monocytes from BD patients.

Bioinformatic findings. Bioinformatic assessment revealed an enrichment of genes and pathways associated with cytoskeletal remodeling among genes that were differentially methylated in monocytes from BD patients versus healthy controls, and GO term analysis using DAVID software revealed significant en-

Table 2. CpG sites that were differentially methylated in CD4+ T cells from Behçet's disease patients compared to CD4+ T cells from healthy controls*

Probe	Gene symbol	Gene name	Methylation (β), patients	Methylation (β), controls	$\Delta\beta$	P
Hypomethylated sites						
cg18404925	*RAC1*	Cell migration–inducing gene 5 protein	0.106	0.308	−0.202	1.79×10^{-34}
cg17509989	*RGS14*	Regulator of G protein signaling 14	0.343	0.545	−0.201	1.42×10^{-27}
cg00103771	*HLA-DRB6*	Major histocompatibility complex, class II, DRβ6	0.453	0.644	−0.192	3.28×10^{-25}
cg06559318	*HLA-DRB6*	Major histocompatibility complex, class II, DRβ6	0.265	0.448	−0.183	2.85×10^{-24}
cg16006841	*RGS14*	Regulator of G-protein signaling 14	0.507	0.678	−0.171	1.02×10^{-20}
cg27362989	*HLA-DRB5*	Major histocompatibility complex, class II, DRβ5	0.322	0.489	−0.167	1.05×10^{-18}
cg23646109	*BCYRN1*, *GJB1*	Brain cytoplasmic RNA 1; gap junction protein, β1, 32 kd	0.737	0.897	−0.160	1.79×10^{-34}
cg01778345	*GDAP2*	Ganglioside-induced differentiation–associated protein 2	0.485	0.630	−0.145	1.6×10^{-13}
cg19516921	*HLA-DRB5*	Major histocompatibility complex, class II, DRβ5	0.326	0.470	−0.144	2.08×10^{-13}
cg06060754	*RGS14*	Regulator of G protein signaling 14	0.475	0.612	−0.137	6.29×10^{-12}
Hypermethylated sites						
cg16474696	*MRI1*	Methylthioribose-1-phosphate isomerase 1; mediator of RhoA-dependent invasion	0.430	0.244	0.186	1.02×10^{-34}
cg08684580	*BAIAP2L1*	Brain-specific angiogenesis inhibitor 1–associated protein 2–like 1	0.444	0.268	0.176	1.02×10^{-34}
cg24634471	*JRK*	Jerky homolog (mouse)	0.564	0.390	0.174	1.02×10^{-34}
cg07796016	*LCE1C*	Late cornified envelope 1C	0.755	0.596	0.158	1.02×10^{-34}
cg04798314	*SMYD3*	SET and MYND domain–containing 3	0.705	0.550	0.155	1.02×10^{-34}
cg16913477	*C3orf39*	Chromosome 2 open-reading frame	0.898	0.758	0.141	1.02×10^{-34}
cg00501169	*NBPF4*	Neuroblastoma breakpoint family, member 4	0.811	0.672	0.139	1.02×10^{-34}
cg10596483	*JRK*	Jerky homolog (mouse)	0.485	0.346	0.139	3.39×10^{-12}
cg26679884	*TUBB8*	Tubulin, β8 class VIII	0.455	0.317	0.138	1.75×10^{-12}
cg25755428	*MRI1*	Methylthioribose-1-phosphate isomerase 1; mediator of RhoA-dependent invasion	0.238	0.100	0.138	1.02×10^{-34}

* The sites listed are those that were the most highly hypo- or hypermethylated in patients compared to controls.

richment of genes related to cytoskeletal dynamics and function among these 228 genes (Table 3). Specifically, genes in the cytoskeletal protein binding, actin cytoskeleton, and M band categories (MF 0008092, CC 0015629, and CC 0031430, respectively) showed the most significant enrichment among genes that were differentially methylated in monocytes.

Among the 62 genes that were differentially methylated in CD4+ T cells, the most prominent according to GO term analysis were related to antigen processing and presentation, with this finding driven primarily by differential methylation in 3 loci within the HLA class II region (Table 4). Enrichment of genes associated with cytoskeletal processes was also observed in CD4+ T cells, but to a lesser degree than in monocytes. In CD4+ T cells, actin cytoskeleton (CC 0015629), cytoskeletal regulation by Rho GTPase (PANTHER P00016), and cytoskeletal protein binding (MF 0008092) were all significantly enriched (FDR < 0.20).

Differential methylation of genes associated with cytoskeletal remodeling. The set of differentially methylated CpG sites in monocytes and CD4+ T cells from patients with BD compared to healthy controls included CpG sites in genes that are involved in multiple levels of cytoskeletal regulation, structure, and function (Supplementary Tables 4 and 5 and Supplementary Figures 1 and 2 [http://onlinelibrary.wiley.com/doi/10.1002/art.38409/abstract]). Differential methylation of Rho GTPase genes, which play a central role in regulating actin cytoskeletal remodeling (21), was observed in CD4+ T cells. *RAC1* (probe cg18404925) exhibited the highest degree of hypomethylation ($\beta = 0.106$ [patients]

Table 3. Gene ontology analysis of CpG sites that were differentially methylated in monocytes from Behçet's disease patients compared to monocytes from healthy controls*

Category	Description	Genes	*P*	FDR, %
MF: 0008092	Cytoskeletal protein binding	*OBSCN*, *MYH15*, *SSH1*, *MYO1C*, *FSCN2*, *BAIAP2L1*, *BAIAP2*, *MYO1D*, *RPH3AL*, *SYNPO2*, *HOMER2*, *TNNI2*, *MPRIP*, *KIF1B*, *ANK1*	0.0024	3.37
CC: 0015629	Actin cytoskeleton	*MYH15*, *FSCN2*, *MYO1C*, *MYO1D*, *FERMT1*, *SYNPO2*, *SLC9A3R1*, *BMF*, *FILIP1L*, *TNNI2*	0.0037	4.75
CC: 0031430	M band	*OBSCN*, *ANK1*, *ENO1*	0.0044	5.59
CC: 0016459	Myosin complex	*MYH15*, *MYO1C*, *MYO1D*, *BMF*, *FILIP1L*	0.0064	8.04
CC: 0030016	Myofibril	*HDAC4*, *OBSCN*, *ANK1*, *MYH15*, *TNNI2*, *ENO1*	0.0088	10.87
MF: 0008093	Cytoskeletal adaptor activity	*ANK1*, *BAIAP2L1*, *BAIAP2*	0.0097	12.92
CC: 0005737	Cytoplasm	*TGOLN2*, *MYH15*, *CHMP6*, *C16ORF70*, *MIPEP*, *CUL3*, *NLRC4*, *ANK1*, *EDARADD*, *BSG*, *BCL2L14*, *BAIAP2*, *HAL*, *PDE4D*, *RPTOR*, *NPC1*, *ATP2C1*, *TRIM34*, *PCMTD1*, *FILIP1L*, *ANKFY1*, *MCTS1*, *TRIM39*, *SH3GL1*, *SSH1*, *PFKFB3*, *GNE*, *CLU*, *CALR*, *AZI1*, *SCRIB*, *ADAP1*, *JRK*, *ARG1*, *LPCAT1*, *GALNS*, *DHODH*, *RNF11*, *DYRK4*, *GLO1*, *TRAF6*, *BMF*, *TEC*, *B4GALT5*, *PTPN7*, *OBSCN*, *UAP1*, *ABR*, *MYO1C*, *NXF2*, *RPS9*, *SULT6B1*, *HOMER2*, *MPRIP*, *TNNI2*, *HDAC4*, *LASS3*, *HIVEP3*, *COPS2*, *MAD1L1*, *FERMT1*, *IL4I1*, *CD93*, *CHST12*, *TRIM6*, *CHST15*, *ACAD8*, *GOLGA3*, *PIGY*, *RPH3AL*, *ARHGAP24*, *PRKCB*, *EML4*, *EIF4G1*, *KIF1B*, *HIPK3*, *LRMP*, *GNAS*, *PCYOX1*, *TRIM6-TRIM34*, *SEC14L1*, *STK40*, *DAPP1*, *CCS*, *ETV6*, *PCSK6*, *EXOC2*, *ENO1*, *FAM125B*, *NXF2B*, *SYNPO2*, *PARK2*, *STAB2*, *CSGALNACT1*, *MRPL21*, *RPS6KA2*, *TRPC4AP*, *CYP4F3*, *RAB38*, *SLC15A4*, *VPS28*, *ACSM5*, *CBS*	0.011	13.81
CC: 0043292	Contractile fiber	*HDAC4*, *OBSCN*, *ANK1*, *MYH15*, *TNNI2*, *ENO1*	0.012	15.07
CC: 0005856	Cytoskeleton	*MAD1L1*, *MYH15*, *SSH1*, *GNE*, *DNAH3*, *FERMT1*, *AZI1*, *ANK1*, *BMF*, *DLG2*, *FSCN2*, *MYO1C*, *MYO1D*, *NXF2B*, *NXF2*, *SYNPO2*, *PDE4D*, *SLC9A3R1*, *ARHGAP24*, *HOMER2*, *RGS14*, *TNNI2*, *MPRIP*, *EML4*, *KIF1B*, *TBCD*, *FILIP1L*	0.014	16.44
CC: 0031672	A band	*OBSCN*, *ANK1*, *ENO1*	0.014	16.72
BP: 0009225	Nucleotide-sugar metabolic process	*CSGALNACT1*, *UAP1*, *GNE*	0.012	18.04
CC: 0005802	Trans-Golgi network k	*TGOLN2*, *ATP2C1*, *C16ORF70*, *GNAS*	0.015	18.32
MF: 0003779	Actin binding	*MYH15*, *SSH1*, *FSCN2*, *MYO1C*, *BAIAP2L1*, *MYO1D*, *SYNPO2*, *HOMER2*, *TNNI2*, *MPRIP*	0.015	18.75
CC: 0012505	Endomembrane system	*MAD1L1*, *BSG*, *BCL2L14*, *PIGY*, *MYO1C*, *CHMP6*, *C16ORF70*, *RPH3AL*, *CSGALNACT1*, *NPC1*, *KIF1B*, *ATP2C1*, *CHST12*, *LRMP*, *GNAS*, *CYP4F3*, *GOLGA3*	0.017	19.91

* FDR = false discovery rate; MF = molecular function; CC = cellular component; BP = biologic process.

and 0.308 [controls]) in CD4+ T cells from patients with BD. *RAC1* regulates T lymphocyte adhesion via integrin and controls actin cytoskeletal dynamics (22,23). Hypermethylation of the gene that encodes RhoJ was also observed in CD4+ T cells from BD patients. Further, *ARHGAP24,* a Rho GTP–associated protein, was hypermethylated in BD patient monocytes.

Differential methylation of genes involved in actin processing, including *FSCN2*, *BAIAP2L1*, *FILIP1L*, and *SSH1*, was demonstrated in monocytes from patients with BD. Hypermethylation of *BAIAP2L1* and hypomethylation of *FSCN2* were observed in monocytes and CD4+ T cells from these patients (Figure 1B and Supplementary Tables 4 and 5). *ANK1*, coding for ankyrin 1, is associated with attachment of integral membrane proteins to the actin cytoskeleton and was also hypermethylated in monocytes from BD patients compared to healthy controls.

Altered methylation of nonmuscle myosin genes was detected in both monocytes and CD4+ T cells from BD patients compared to controls. We observed hypermethylation of myosin heavy chain 15 (*MYH15*) in

Table 4. Gene ontology analysis of CpG sites that were differentially methylated in CD4+ T cells from Behçet's disease patients compared to CD4+ T cells from healthy controls*

Category	Description	Genes	*P*	FDR, %
KEGG: hsa05310	Asthma	*HLA-DQB1*, *EPX*, *PRG2*, *HLA-DRB5*, *HLA-DQA1*	8.21×10^{-7}	7.42×10^{-4}
KEGG: hsa05416	Viral myocarditis	*HLA-DQB1*, *MYH15*, *RAC1*, *HLA-DRB5*, *HLA-DQA1*	3.14×10^{-5}	0.0284
KEGG: hsa04612	Antigen processing and presentation	*HLA-DQB1*, *HLA-DRB5*, *NFYA*, *HLA-DQA1*	0.0013	1.21
CC: 0042613	Class II MHC protein complex	*HLA-DQB1*, *HLA-DRB5*, *HLA-DQA1*	0.0029	3.32
KEGG: hsa05330	Allograft rejection	*HLA-DQB1*, *HLA-DRB5*, *HLA-DQA1*	0.0042	3.74
KEGG: hsa05332	Graft-versus-host disease	*HLA-DQB1*, *HLA-DRB5*, *HLA-DQA1*	0.0049	4.36
KEGG: hsa04940	Type 1 diabetes mellitus	*HLA-DQB1*, *HLA-DRB5*, *HLA-DQA1*	0.0057	5.03
BP: 0002504	Antigen processing and presentation of peptide or polysaccharide antigen via class II MHC	*HLA-DQB1*, *HLA-DRB5*, *HLA-DQA1*	0.0043	6.06
KEGG: hsa04672	Intestinal immune network for IgA production	*HLA-DQB1*, *HLA-DRB5*, *HLA-DQA1*	0.0077	6.74
CC: 0015629	Actin cytoskeleton	*MYH15*, *FSCN2*, *MYOM2*, *FERMT1*, *TNNI2*	0.0064	7.18
KEGG: hsa05320	Autoimmune thyroid disease	*HLA-DQB1*, *HLA-DRB5*, *HLA-DQA1*	0.0083	7.26
OMIM	Celiac disease, susceptibility to	*HLA-DQB1*, *HLA-DQA1*	0.011	8.60
CC: 0043234	Protein complex	*HLA-DQB1*, *MYH15*, *TOLLIP*, *FERMT1*, *NFYA*, *HLA-DQA1*, *GJB1*, *TNNI2*, *MYOM2*, *HLA-DRB5*, *TUBB8*, *IFFO1*, *NCOR2*, *GOLGA3*, *GABRP*	0.008	8.90
PANTHER: P00016	Cytoskeletal regulation by Rho GTPase	*RHOJ*, *MYH15*, *RAC1*, *TUBB8*	0.012	9.00
CC: 0042611	MHC protein complex	*HLA-DQB1*, *HLA-DRB5*, *HLA-DQA1*	0.011	11.90
CC: 0032991	Macromolecular complex	*HLA-DQB1*, *MYH15*, *TOLLIP*, *FERMT1*, *NFYA*, *HLA-DQA1*, *GJB1*, *TNNI2*, *JRK*, *MYOM2*, *HLA-DRB5*, *TUBB8*, *IFFO1*, *GOLGA3*, *NCOR2*, *GABRP*	0.019	19.77
MF: 0008092	Cytoskeletal protein binding	*MYH15*, *FSCN2*, *BAIAP2L1*, *FRMD4A*, *RPH3AL*, *TNNI2*	0.018	19.79

* KEGG = Kyoto Encyclopedia of Genes and Genomes; MHC = major histocompatibility complex (see Table 3 for other definitions).

monocytes and CD4+ T cells. In monocytes, we further observed hypomethylation of myosin 1C, (*MYO1C*) and hypermethylation of *MYO1D* and *MPRIP* (Supplementary Table 4).

Differential methylation of genes encoding microtubule-related proteins was also found in both cell types. Hypomethylation of *TBCD*, *KIF1B*, and *DNAH3* was detected in monocytes, and *TUBB8* was hypermethylated in BD patient CD4+ T cells compared to controls (Figure 1B and Supplementary Tables 4 and 5). In both monocytes and CD4+ T cells there was significant hypomethylation of multiple CpG sites in *RGS14*, a gene that encodes a microtubule-associated protein (24) (Figure 1B and Supplementary Tables 4 and 5).

Alteration of DNA methylation in microtubule processing genes after treatment for Behçet's disease. We found widespread differences in DNA methylation between monocytes and CD4+ T cells from untreated BD patients with active disease and samples obtained from the same patients following treatment and achievement of disease remission. A lower threshold for DNA methylation differences ($\Delta\beta \geq 0.05$) was applied to enable detection of smaller changes in DNA methylation and partial restoration (by at least 50%) of the DNA methylation changes observed in patients with BD. We detected a total of 1,426 differentially methylated CpG sites in monocytes after treatment; of these, 636 were hypomethylated and 790 were hypermethylated. In CD4+ T cells, a total of 2,044 CpG sites were differentially methylated following treatment, with 1,012 hypomethylated and 1,032 hypermethylated.

Bioinformatic analysis of genes that displayed differential methylation in BD patients following treatment revealed enrichment of genes in multiple GO categories, including some that are related to microtubules, in both cell types (Supplementary Table 6 [on the *Arthritis & Rheumatology* web site at http://onlinelibrary.wiley.com/doi/10.1002/art.38409/abstract]). In monocytes, microtubule cytoskeleton (CC 0015630), microtubule organizing center (CC 0005815), cytoskeleton

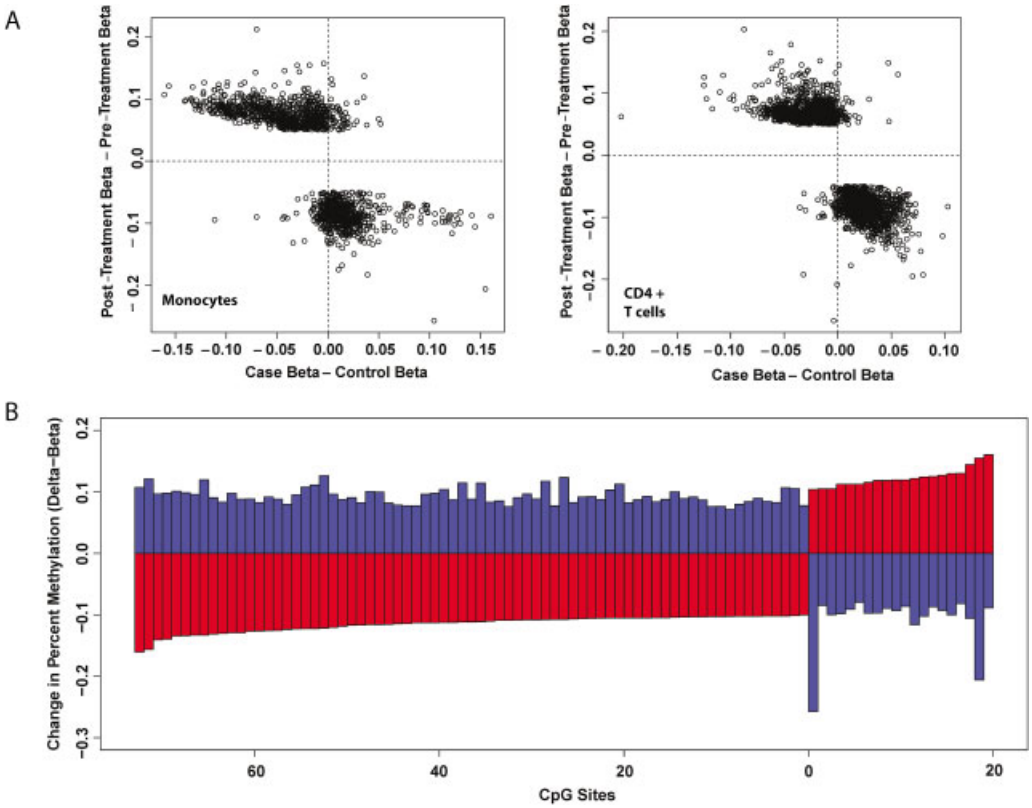

Figure 2. Reversal of changes in DNA methylation in Behçet's disease (BD) patients following treatment. **A,** CpG sites that were differentially methylated in individual BD patients after versus before treatment (differential score ≥ 22, $\Delta\beta \geq 0.05$), plotted according to the differences in DNA methylation observed between BD patients and healthy controls (x-axes) and the change in methylation upon treatment (y-axes). In each panel, CpG sites that were hypomethylated in BD patients are represented on the left of the vertical dashed line, and hypermethylated sites on the right. CpG sites with increased and decreased methylation following treatment are represented above and below the horizontal dashed line, respectively. CpG sites in the upper left and lower right quadrants are those in which treatment acted to reverse differences between BD patients and controls. Enrichment of treatment-responsive CpG sites in the upper left and lower right quadrants of the plots demonstrates that treatment-induced reversal of BD methylation differences occurred frequently. **B,** Methylation changes in differentially methylated CpG sites in BD patient monocytes that also displayed differential methylation in individual patients after disease remission was achieved. There were a total of 94 such sites, and in 93 of these (represented in the figure), the direction of methylation change in individual patients after versus before remission was opposite to the direction of change observed between patients and controls. Red bars represent the difference in percent methylation between patients and controls; blue bars represent the difference in percent methylation on the same CpG sites in patients after achievement of disease remission compared to the same patients before treatment.

organization (BP 0007010), and cytoskeleton (CC 0005856) genes were enriched. Microtubule cytoskeleton was also among the top 20 terms obtained in GO term analysis of CD4+ T cells after treatment.

Altered methylation of genes associated with microtubule structure and organization was found in both monocytes and CD4+ T cells following treatment (Supplementary Tables 7 and 8). Hypomethylation of tubulin genes *TUBA3C* and *TUBA3D* and tubulin polymerizing promoting protein (*TPPP)* was observed after treatment of BD and achievement of disease remission. Further, we observed significant alteration of the methylation of kinesin and dynein genes in both monocytes and CD4+ T cells. *KIF2A* was hypermethylated in both cell types following treatment.

Treatment-induced reversal of DNA methylation changes in monocytes and CD4+ T cells from Behçet's disease patients. Alterations in DNA methylation patterns occurring in BD patients after achievement of disease remission were found to counteract DNA methylation differences between BD patients and healthy controls that had been observed pretreatment. Among CpG sites that were differentially methylated after treatment versus before, there was almost exclusive reversal of the direction of aberrant methylation demonstrated between patients and controls (Figure 2A). In a com-

parison of methylation differences identified between BD patients and healthy controls and those detected within individual BD patients before and after treatment, there were 94 overlapping CpG sites among 69 genes in monocytes and 9 overlapping CpG sites among 7 genes in CD4+ T cells. In both cell types, treatment reversed BD-associated differences in DNA methylation. In 93 of the 94 CpG sites that displayed differences in BD monocytes following treatment, the direction of methylation change was opposite to that observed between BD patients and controls (Figure 2B). In many cases DNA methylation in BD patients was completely restored following treatment, to levels similar to those in controls (Supplementary Table 9 [http://onlinelibrary.wiley.com/doi/10.1002/art.38409/abstract]).

DISCUSSION

In this first reported epigenomic study of BD, we have obtained evidence of widespread and reversible patterns of altered DNA methylation in this disease. Of particular interest, epigenetic dysregulation in BD was evident across multiple levels of cytoskeletal organization including actin binding, Rho GTPase enzymes, motor proteins, and microtubule structure. Cytoskeletal rearrangement is a process involved in locomotion, focal adhesion, and cellular proliferation in leukocytes. Our data suggest that aberrant epigenetic regulation of cytoskeletal remodeling genes in BD might underlie the increased leukocyte migration and tissue infiltration central to pathogenesis of the disease.

Among the differentially methylated genes detected in BD, we demonstrated hypomethylation of cytoskeletal genes implicated in increased chemotaxis in normal lymphocytes and invadopodia formation in cancer. Fascin plays a central role in filopodia formation and potentiates invasive migration of cancer cells (25,26), and we observed hypomethylation of fascin actin-bundling protein 2 (*FSCN2*) in monocytes and CD4+ T cells from patients with BD. Hypomethylation of *SSH1*, a cofilin-phosphatase that regulates actin filament dynamics of cell migration (27), was found in monocytes, but not CD4+ T cells, from BD patients. In monocytes and CD4+ T cells, we demonstrated hypermethylation of *BAIAP2L1* (IRTKS), which functions in actin bundling and cell migration (28,29).

In CD4+ T cells, *RAC1* displayed the highest level of hypomethylation in BD patients compared to controls. Further, partial restoration of reduced *RAC1* methylation was observed in patients after achievement of disease remission. Differential methylation of *RAC1* accessory proteins including the actin regulatory protein *ARHGAP24*, which functions to reduce expression of *Rac1* and *Cdc42* in murine podocytes (30), was also detected in monocytes from BD patients. *MPRIP*, which was hypermethylated in BD patient monocytes, is involved in the formation of actin structures that are involved in T cell migration through the activation of Rac1 (31). We observed hypermethylation of synaptojanin 2 (*SYNJ2*), a Rac1 effector that regulates clathrin-mediated endocytosis and invadopodia formation (32), in BD patient monocytes and CD4+ T cells following treatment.

In lymphocytes, myosin motor proteins perform a variety of cellular functions including regulation of the cytoskeleton, projections of the cell surface, and cell membrane processes (e.g., phagocytosis) (33). Myosin light chain phosphorylation influences monocyte migration through the endothelial barrier (34). Class II myosins play a role in cell motility through regulating actin polymerization in the formation of lamellipodia. Nonmuscle myosin heavy chain IIA (*MYH9*) is involved in abrogation of T cell motility upon antigen recognition and focal adhesion (35). In BD monocytes, we observed hypermethylation of obscurin (*OBSCN*) and *ANK1*. Obscurin is involved in myofibril organization through its regulation of TC10 (RhoQ) and also interacts with *ANK1* (36,37). *MYH15* was hypermethylated in BD monocytes and CD4+ T cells. In addition, altered methylation of myomesin 2 (*MYOM2*) was observed in BD CD4+ T cells.

Immune complex formation might be involved in the pathogenesis of BD (38). Interestingly, cytoskeletal components are frequent targets for autoantibody formation in BD, and antibodies recognizing intermediate filaments of the cytoskeleton have been observed (39). Further, autoantibodies targeting cofilin 1, tubulin-like, and actin-like self antigens have been demonstrated in a subset of patients (40).

We examined the effect of treatment and disease remission on DNA methylation changes in monocytes and CD4+ T cells from patients with BD. Colchicine is commonly used as a first-line treatment for mucocutaneous manifestations of BD and was the primary medication used to manage the disease in the patients included in this study. The effectiveness of colchicine in limiting the severity of BD is thought to be due to its ability to attenuate leukocyte chemotaxis (41). Colchicine is known to limit cell motility through the disruption of microtubule organization and structure. Consistent with this known effect, a number of genes related to microtubule formation and organization were differentially methylated in both monocytes and CD4+ T cells

from BD patients following colchicine treatment. Hypermethylation of the kinesin gene *KIF2A* and hypomethylation of *TPPP* were observed in monocytes and CD4+ T cells from treated patients. Interestingly, kinesin deficiency results in weakened intercellular adhesion without affecting adherens junction components at the plasma membrane (42). Up-regulation of *TPPP* has been reported to induce altered microtubule structure and reduce cell viability (43).

In BD monocytes we observed hypomethylation of tubulin folding cofactor D (*TBCD*), which was reversed upon treatment. Similarly, hypomethylation of tripartite motif containing 39 (*TRIM39*) in BD monocytes was reversed following treatment. A genetic association between *TRIM39*, which encodes a RING domain–containing E3 ubiquitin ligase, and BD has been previously reported in a Japanese population (44). Of interest, we also detected hypomethylation of *UBAC2*, which encodes a protein with a ubiquitin-associated domain, in BD patient monocytes, suggesting a role of this gene product in ubiquitination pathways. *UBAC2* is a confirmed genetic susceptibility locus in BD, and the risk allele in this locus has been shown to be associated with increased *UBAC2* messenger RNA expression in PBMCs (45). The DNA hypomethylation detected in *UBAC2* was almost completely restored upon disease remission in our patients. Differential methylation in several HLA class II loci was notable primarily in CD4+ T cells from patients with BD. Specifically, hypomethylation across several CpG sites in *HLA-DRB5* and *HLA-DRB6* was observed. There is currently no strong evidence supporting the presence of a genetic susceptibility locus within HLA class II in BD, despite the demonstration of multiple independent susceptibility loci located within HLA class I (12).

In summary, the current results provide evidence of epigenetic remodeling and reversal of specific DNA methylation changes following the achievement of remission in an inflammatory disease. This emphasizes the potential for epigenetic studies to reveal novel aspects of disease pathogenesis, which might lead to the identification of new targets for disease monitoring and treatment. Our findings strongly support the notion that dynamic and reversible epigenetic changes in cytoskeletal remodeling genes play an important role in the pathogenesis of BD. We have demonstrated that following treatment, BD-associated variations in DNA methylation undergo epigenetic remodeling, with reversal of DNA methylation differences observed between BD patients and controls. DNA methylation changes that are restored upon disease remission represent potential biomarkers for disease activity and treatment responsiveness in BD. A large longitudinal study will be necessary to fully explore the utility of these altered DNA methylation changes as biomarkers. Future investigations to characterize the capacity of specific DNA methylation changes in BD and other inflammatory and autoimmune diseases to predict disease manifestations, clinical course, and response to treatment are warranted.

AUTHOR CONTRIBUTIONS

All authors were involved in drafting the article or revising it critically for important intellectual content, and all authors approved the final version to be published. Dr. Sawalha had full access to all of the data in the study and takes responsibility for the integrity of the data and the accuracy of the data analysis.

Study conception and design. Hughes, Ture-Ozdemir, Alibaz-Oner, Direskeneli, Sawalha.

Acquisition of data. Hughes, Ture-Ozdemir, Alibaz-Oner, Coit, Direskeneli, Sawalha.

Analysis and interpretation of data. Hughes, Ture-Ozdemir, Alibaz-Oner, Coit, Direskeneli, Sawalha.

REFERENCES

1. Muller W, Lehner T. Quantitative electron microscopical analysis of leukocyte infiltration in oral ulcers of Behçet's syndrome. Br J Dermatol 1982;106:535–44.
2. Sahin S, Lawrence R, Direskeneli H, Hamuryudan V, Yazici H, Akoglu T. Monocyte activity in Behçet's disease. Rheumatology 1996;35:424–9.
3. Kim W, Do J, Park K, Cho M, Park S, Cho C, et al. Enhanced production of macrophage inhibitory protein-1α in patients with Behçet's disease. Scand J Rheumatol 2004;34:129–35.
4. Geri G, Terrier B, Rosenzwajg M, Wechsler B, Touzot M, Seilhean D, et al. Critical role of IL-21 in modulating T_H17 and regulatory T cells in Behçet disease. J Allergy Clin Immunol 2011;128:655–64.
5. Suzuki Y, Hoshi K, Matsuda T, Mizushima Y. Increased peripheral blood $\gamma\delta^+$ T cells and natural killer cells in Behçet's disease. J Rheumatol 1992;19:588–92.
6. Parlakgul G, Guney E, Erer B, Kilicaslan Z, Direskeneli H, Gul A, et al. Expression of regulatory receptors on $\gamma\delta$ T cells and their cytokine production in Behçet's disease. Arthritis Res Ther 2013;15:R15.
7. Triolo G, Accardo-Palumbo A, Triolo G, Carbone MC, Ferrante A, Giardina E. Enhancement of endothelial cell E-selectin expression by sera from patients with active Behçet's disease: moderate correlation with anti-endothelial cell antibodies and serum myeloperoxidase levels. Clin Immunol 1999;91:330–7.
8. Niwa Y, Miyake S, Sakane T, Shingu M, Yokoyama M. Autooxidative damage in Behçet's disease—endothelial cell damage following the elevated oxygen radicals generated by stimulated neutrophils. Clin Exp Immunol 1982;49:247–55.
9. Ivanov AI, McCall IC, Parkos CA, Nusrat A. Role for actin filament turnover and a myosin II motor in cytoskeleton-driven disassembly of the epithelial apical junctional complex. Mol Biol Cell 2004;15:2639–51.
10. Ivanov AI, Parkos CA, Nusrat A. Cytoskeletal regulation of epithelial barrier function during inflammation. Am J Pathol 2010;177:512–24.
11. Verity D, Marr J, Ohno S, Wallace G, Stanford M. Behçet's disease, the Silk Road and HLA-B51: historical and geographical perspectives. Tissue Antigens 1999;54:213–20.

12. Hughes T, Coit P, Adler A, Yilmaz V, Aksu K, Duzgun N, et al. Identification of multiple independent susceptibility loci in the HLA region in Behçet's disease. Nat Genet 2013;45:319–24.
13. Gul A. Genetics of Behçet's disease: lessons learned from genome-wide association studies. Curr Opin Rheumatol 2014;26:56–63.
14. Coit P, Jeffries M, Altorok N, Dozmorov MG, Koelsch KA, Wren JD, et al. Genome-wide DNA methylation study suggests epigenetic accessibility and transcriptional poising of interferon-regulated genes in naive CD4+ T cells from lupus patients. J Autoimmun 2013;43:78–84.
15. Altorok N, Coit P, Hughes T, Koelsch KA, Stone DU, Rasmussen A, et al. Genome-wide DNA methylation patterns in naive CD4+ T cells from patients with primary Sjögren's syndrome. Arthritis Rheum 2014;66:731–9.
16. De la Rica L, Urquiza JM, Gomez-Cabrero D, Islam AB, Lopez-Bigas N, Tegner J, et al. Identification of novel markers in rheumatoid arthritis through integrated analysis of DNA methylation and microRNA expression. J Autoimmun 2013;41:6–16.
17. Sunahori K, Nagpal K, Hedrich CM, Mizui M, Fitzgerald LM, Tsokos GC. The catalytic subunit of protein phosphatase 2A (PP2Ac) promotes DNA hypomethylation by suppressing the phosphorylated mitogen-activated protein kinase/extracellular signal-regulated kinase (ERK) kinase (MEK)/phosphorylated ERK/DNMT1 protein pathway in T-cells from controls and systemic lupus erythematosus patients. J Biol Chem 2013;288:21936–44.
18. Sawalha AH. Epigenetics and T-cell immunity. Autoimmunity 2008;41:245–52.
19. Huang DW, Sherman BT, Lempicki RA. Systematic and integrative analysis of large gene lists using DAVID bioinformatics resources. Nat Protoc 2008;4:44–57.
20. Warde-Farley D, Donaldson SL, Comes O, Zuberi K, Badrawi R, Chao P, et al. The GeneMANIA prediction server: biological network integration for gene prioritization and predicting gene function. Nucleic Acids Res 2010;38:W214–20.
21. Heasman SJ, Ridley AJ. Mammalian Rho GTPases: new insights into their functions from in vivo studies. Nat Rev Mol Cell Biol 2008;9:690–701.
22. D'Souza-Schorey C, Boettner B, van Aelst L. Rac regulates integrin-mediated spreading and increased adhesion of T lymphocytes. Mol Cell Biol 1998;18:3936–46.
23. Tapon N, Hall A. Rho, Rac and Cdc42 GTPases regulate the organization of the actin cytoskeleton. Curr Opin Cell Biol 1997;9:86–92.
24. Martin-McCaffrey L, Willard FS, Pajak A, Dagnino L, Siderovski DP, D'Souza SJ. RGS14 is a microtubule-associated protein. Cell Cycle 2005;4:953–60.
25. Li A, Dawson JC, Forero-Vargas M, Spence HJ, Yu X, Konig I, et al. The actin-bundling protein fascin stabilizes actin in invadopodia and potentiates protrusive invasion. Curr Biol 2010;20:339–45.
26. Vignjevic D, Kojima S, Aratyn Y, Danciu O, Svitkina T, Borisy GG. Role of fascin in filopodial protrusion. J Cell Biol 2006;174:863–75.
27. Huang TY, DerMardirossian C, Bokoch GM. Cofilin phosphatases and regulation of actin dynamics. Curr Opin Cell Biol 2006;18:26–31.
28. Millard TH, Dawson J, Machesky LM. Characterisation of IRTKS, a novel IRSp53/MIM family actin regulator with distinct filament bundling properties. J Cell Sci 2007;120:1663–72.
29. Chen G, Li T, Zhang L, Yi M, Chen F, Wang Z, et al. Src-stimulated IRTKS phosphorylation enhances cell migration. FEBS Lett 2011;585:2972–8.
30. Akilesh S, Suleiman H, Yu H, Stander MC, Lavin P, Gbadegesin R, et al. Arhgap24 inactivates Rac1 in mouse podocytes, and a mutant form is associated with familial focal segmental glomerulosclerosis. J Clin Invest 2011;121:4127–37.
31. Sala-Valdes M, Gordon-Alonso M, Tejera E, Ibanez A, Cabrero JR, Ursa A, et al. Association of syntenin-1 with M-RIP polarizes Rac-1 activation during chemotaxis and immune interactions. J Cell Sci 2012;125:1235–46.
32. Chuang Y, Tran NL, Rusk N, Nakada M, Berens ME, Symons M. Role of synaptojanin 2 in glioma cell migration and invasion. Cancer Res 2004;64:8271–5.
33. Maravillas-Montero JL, Santos-Argumedo L. The myosin family: unconventional roles of actin-dependent molecular motors in immune cells. J Leukoc Biol 2012;911:35–46.
34. Haidari M, Zhang W, Chen Z, Ganjehei L, Warier N, Vanderslice P, et al. Myosin light chain phosphorylation facilitates monocyte transendothelial migration by dissociating endothelial adherens junctions. Cardiovasc Res 2011;92:456–65.
35. Jacobelli J, Chmura SA, Buxton DB, Davis MM, Krummel MF. A single class II myosin modulates T cell motility and stopping, but not synapse formation. Nat Immunol 2004;5:531–8.
36. Coisy-Quivy M, Touzet O, Bourret A, Hipskind RA, Mercier J, Fort P, et al. TC10 controls human myofibril organization and is activated by the sarcomeric RhoGEF obscurin. J Cell Sci 2009;122:947–56.
37. Bagnato P, Barone V, Giacomello E, Rossi D, Sorrentino V. Binding of an ankyrin-1 isoform to obscurin suggests a molecular link between the sarcoplasmic reticulum and myofibrils in striated muscles. J Cell Biol 2003;160:245–53.
38. Williams B, Lehner T. Immune complexes in Behçet's syndrome and recurrent oral ulceration. Br Med J 1977;1:1387–9.
39. Akoglu T, Kozakoglu H, Akoglu E. Antibody to intermediate filaments of the cytoskleton in patients with Behçet's disease. Clin Immunol Immunopathol 1986;41:427–32.
40. Ooka S, Nakano H, Matsuda T, Okamoto K, Suematsu N, Kurokawa MS, et al. Proteomic surveillance of autoantigens in patients with Behçet's disease by a proteomic approach. Microbiol Immunol 2010;54:354–61.
41. Jorizzo JL, Hudson RD, Schmalstieg FC, Daniels JC, Apisarnthanarax P, Henry JC, et al. Behçet's syndrome: immune regulation, circulating immune complexes, neutrophil migration, and colchicine therapy. J Am Acad Dermatol 1984;10:205–14.
42. Nekrasova OE, Amargo EV, Smith WO, Chen J, Kreitzer GE, Green KJ. Desmosomal cadherins utilize distinct kinesins for assembly into desmosomes. J Cell Biol 2011;195:1185–203.
43. Lehotzky A, Tirian L, Tokesi N, Lenart P, Szabo B, Kovacs J, et al. Dynamic targeting of microtubules by TPPP/p25 affects cell survival. J Cell Sci 2004;117:6249–59.
44. Kurata R, Nakaoka H, Tajima A, Hosomichi K, Shiina T, Meguro A, et al. TRIM39 and RNF39 are associated with Behçet's disease independently of HLA-B*51 and -A*26. Biochem Biophys Res Commun 2010;401:533–7.
45. Sawalha AH, Hughes T, Nadig A, Yilmaz V, Aksu K, Keser G, et al. A putative functional variant within the UBAC2 gene is associated with increased risk of Behçet's disease. Arthritis Rheum 2011;63:3607–12.